JCAMECH

Vol. 50, No. 2, December 2019, pp 381-386
DOI: 10.22059/jcamech.2019.292736.456

Fluid-structure interaction studies on marine propeller

S. Rama Krishna, V. Gautham Ajay*
Department of Mechanical Engineering, Gayatri Vidya Parishad College of Engineering (Autonomous)
Andrapradesh, Visakhapatnam-530048

ARTICLE INFO

Article history:
Received: 25 November 2019
Accepted: 05 December 2019

Keywords:
Composite Propeller
Carbon/Epoxy
R-Glass/Epoxy
S2-Glass/Epoxy
Hashin Damage Criteria

ABSTRACT

Composite propellers offer high damping characteristics and corrosion resistance when compared with metal propellers. But the design of a hybrid composite propeller with the same strength of metal propeller is the critical task. For this purpose, the present paper focusses on fluid-structure interaction analysis of hybrid composite propeller with Carbon/Epoxy, R-Glass/Epoxy and S2-Glass/Epoxy to find its strength at the same operating conditions of the baseline aluminium propeller. The surface and solid models of the hybrid composite propeller are modelled using modelling software (CATIA) and these models are imported into mesh generation software (Hypermesh) to generate the surface mesh and solid mesh respectively. This surface model of the hybrid composite propeller is imported into computational fluid dynamics software (Fluent) to estimate the pressure loads on propeller blades. These pressure loads from Fluent are imported into FEA software (Abaqus) and applied on the propeller to find the deformation and strength of hybrid composite propeller due to fluid-structure interaction loads. Optimization study is carried out on hybrid composite propeller with different layup sequences of Carbon/R-Glass/S2-Glass to find the optimum strength. From the optimization study, it is found that the hybrid composite propeller with layup-3 of $55^0/55^0/90^0/0^0/0^0/90^0/45^0/90^0/$ $0^0/90^0/45^0/90^0/45^0/90^0/0^0/90^0/0^0$ generates the least stress compared with other layups for the same pressure load obtained from fluid flow simulations. Damage initiation analysis is also carried out on hybrid composite propeller with optimized layup-3 based on Hashin damage criteria and found that the design is safe.

1. Introduction

Marine propeller is a type of fan, it converts rotational motion into thrust by transmitting power. Main part in the propeller is the blade and it is used to convert the rotary motion into forward thrust required to move the vehicle. Present analysis is focussed on redesign of marine propeller blade with hybrid composites to improve the strength, performance in cavitation and noise reduction. Hamzezadea et al. [1] carried the steady state CFD (Computational Fluid Dynamics) simulations using ANSYS on five-stage compressor to study the effect of a single circumferential groove casing treatment on the flow and stability of compressor. Fazel et al. [2] implemented the composite material failure theory into the finite element method software to predict the failure index of adhesive joints. Smith et al. [3] developed the computer program BLADE for generating 3-dimensional propeller blade coordinates with examples of its graphic output. Subhas et al. [4] compared the cavitation simulation results of marine propeller using Fluent with experimental results for validation of simulation methodology used for prediction of cavitation on propeller. Barry [5] explained the basic elements of marine propulsion used for boats and small ships.

Marsh [6] studied the new trends in composite marine propellers and their innovations and found that the composites are the most favourable material for variable pitch propellers and also for corrosion resistive. Rahimi et al. [7] performed the progressive failure analysis of composite structures with the help of numerical tools. Rama Krishna et al. [8] carried out the fluid flow and acoustic analysis of motor fan using Fluent and suggested the design modification for reduction of motor fan noise. Zhang et al. [9] carried out composite laminate analysis for different layup orientation by varying load conditions, material properties and the geometry of the laminate. Progressive failure of carbon/epoxy laminates were simulated and highlight the importance of commercial numerical software [10, 11]. Gorji Mohsen et al. [12] carried CFD simulations using Fluent to obtain hydrodynamic performance and noise of marine propeller at five different operation conditions.

*Corresponding Author: sramakrishna@gvpce.ac.in

Shishesaz et al. [13] performed finite element analysis to study the buckling effect on composite plates and found that stacking sequence has a significant effect on the load carrying capacity of the composite plate. Jiang et al. [15] developed the multi-objective optimization methodology using dominated Sorting Genetic Algorithm to carry out fluid structure interaction analysis on propeller. Maljaars et al. [16] predicted the flexible propeller responses using BEM-FEM and RANS-FEM methods and concluded that BEM-FEM and RANS-FEM coupling can be best method for predict the bending response and these methods are not suggested for computing the twist deformations of composite propeller. Prabhu et al. [17] simulated the fluid structure interaction of marine cycloidal propeller using panel method and found that the unsteady flow and fluid structure coupling have significant impact on the characteristics of the cycloidal propeller blade. Sun et al. [18] predicted the hydro-elastic performance of marine propeller using boundary element method and finite element method. Zelibe et al. [19] investigated the performance of fibre-glass/talc filled epoxy as an insulator by both experimental and numerical methods and suggested that fibre-glass talc filled epoxy can be used as domestic heating insulation. Zelibe et al. [20] used the shape memory alloy to improve the hydrodynamic efficiency of the marine composite propeller. Shape memory alloy was used to control the twist of propeller blade. Kim et al. [21] developed an LST-FEM method to predict the deformation of the blade using fluid-structure interaction analysis and also presented the influence of the lamination direction on the deformation of the flexible composite propeller.

2. Fluid flow analysis

The surface model of propeller with hub, blade, front cone and shaft is generated as per the dimensions taken from the literature [4]. CFD analysis was carried out on the propeller of diameter 200mm with 5 blades as shown in Figure 1. The pressure loads on the blades of propeller were estimated when the inlet velocity of flow is 6.22 m/sec and propeller is rotated at a speed of 780 rpm. The pressure loads are exported into Abaqus for structural analysis to find the strength of composite propeller. For CFD analysis, flow domain is created around the propeller for simulation of pressure loads on the propeller blades. Figure 2 show flow domain of propeller used for present CFD simulations. Origin is considered at the centreline of hub for creation of flow domain around the propeller. Inlet is considered at distance of 600 mm (three times of propeller diameter) towards the nose cone of propeller from the origin, outlet let is considered at distance of 800 mm (four times of propeller diameter) opposite to the nose cone of propeller from the origin and farfield is created around the propeller with diameter of 400 mm (two times of propeller diameter) from the origin.

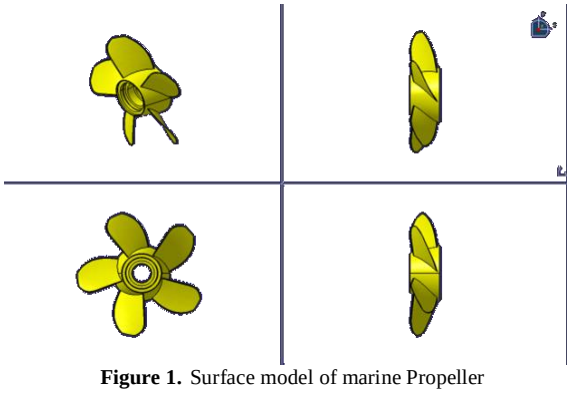

Figure 1. Surface model of marine Propeller

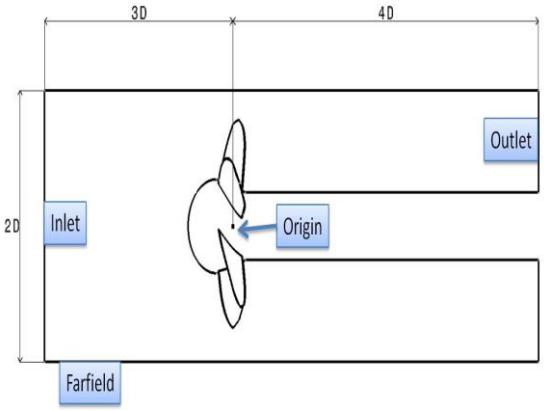

Figure 2. Flow domain of propeller interms of propeller diameter (D)

After creation of surface model of propeller, it is exported into Hypermesh software for generation of surface mesh for fluid flow simulations using Fluent. Mesh generation is another important step for flow analysis using Fluent. Four node quadrilateral element is used for generation of surface mesh for propeller. The 3D tetramesh is generated for farfield with inlet and outlet using CTETRA elements available in the Hypermesh software [14]. Figure 3 and Figure 4 show the surface mesh generated for propeller blade and tetra mesh generated for farfield around propeller respectively.

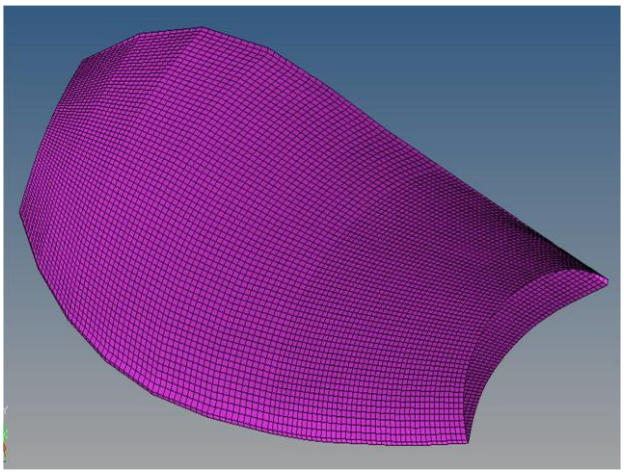

Figure 3. Surface mesh of propeller blade

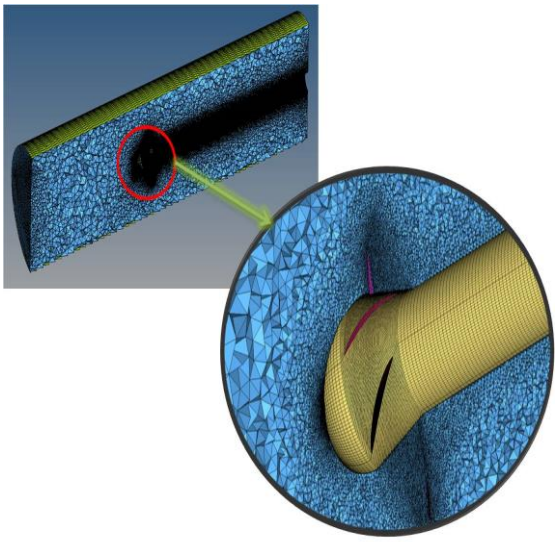

Figure 4. Tetramesh for farfield around the propeller

The meshed model of propeller was imported into Fluent for flow analysis to simulate pressure loads on the propeller blades. Figure 5 show flow domain around the propeller in Fluent for fluid flow analysis. The velocity inlet is selected for inlet and outflow is applied for outlet of farfield of propeller. Turbulent flow around the propeller is simulated using k-epsilon model available in the Fluent. Farfield is taken as fluid and water-liquid properties are assigned to entire domain of propeller. A relative rotational velocity of zero is assigned to wall forming the propeller blade, nose cone and hub. A uniform velocity of 6.22 m/sec is assigned to inlet of farfield along the axis parallel to the shaft of propeller and rotational velocity of 780 rpm is assigned to the fluid in the far field using moving reference frame. Turbulent kinetic energy of 0.0025 m^2/sec^2 and turbulent dissipation rate of 0.001125 m^2/sec^3 is considered for simulation of turbulent flow around the propeller. The advance coefficient of 1.28 and operating pressure of 0.135MPa is considered in the farfield of propeller to initiate flow simulation on propeller to find the pressure loads on the propeller blades.

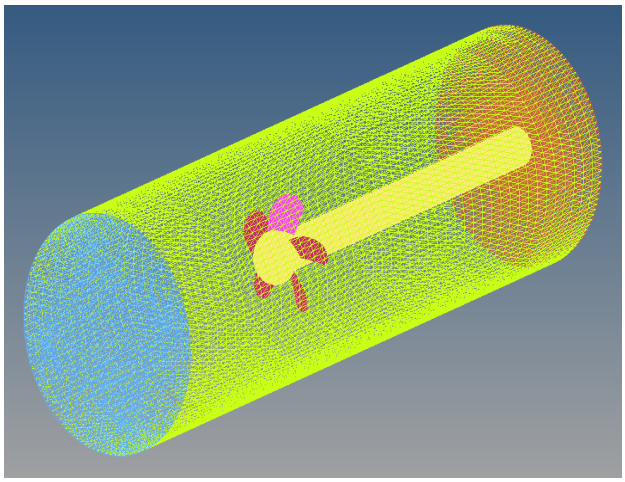

Figure 5 Flow domain around the propeller

3. Fluid structure interaction analysis

Solid model of propeller with hub and blades was generated using CATIA and it was exported into Hypermesh for generation of separate mesh for aluminum propeller and hybrid composite propeller with different ply orientations. The material properties of Young's modulus of 71 GPa and Poisson's ratio of 0.32 are given as input for aluminum propeller in Hypermesh. Table 1 shows the material properties of Carbon/Epoxy, R-Glass/Epoxy and S2-Glass/Epoxy [11]. Each layer with thickness of 0.3 mm is considered for design of layup sequence with 16 layers of hybrid composite propeller. Table 2 shows fiber orientation for layup-1, layup-2 and layup-3 for 16 layers of hybrid composite propeller.

The 3D tetramesh is generated for aluminum propeller and hybrid composite propeller using CTETRA elements available in the Hypermesh. Thickness of blade is changing in both longitudinal and transverse directions. So each layup is considered for generation of mesh for hybrid composite propeller in both longitudinal and transverse directions. Figure 6 and Figure 7 represents the meshed models for aluminum propeller and hybrid composite propeller respectively. The meshed models of aluminum propeller and hybrid composite propeller with three different layup sequences were exported into Abaqus for fluid structure interaction analysis to estimate the strength. Pressure loads are applied on blade surface from root to tip at regular intervals as shown in Figure 8.The deformation of propeller due to fluid pressure was estimated using Abaqus and the deformed propeller was imported into Hypermesh for generation of surface mesh. After completion of mesh, the deformed propeller was again imported into Fluent for estimation of pressure loads. These new pressure loads are used to find strength of hybrid composite marine propeller using Abaqus.

Table 1. Material properties of hybrid composite propeller (Volume fraction of fibre=0.6)

	Carbon/Epoxy	R-Glass/Epoxy	S_2-Glass/Epoxy
E_1 (GPa)	142.0	53.1	22.9
E_2 (GPa)	100.0	12.4	12.4
E_3 (GPa)	100.0	12.4	12.4
G_{12} (GPa)	5.2	6.6	4.7
G_{23} (GPa)	3.8	4.1	4.2
G_{13} (GPa)	3.8	4.1	4.2
ϑ_{12}	0.5	0.32	0.31
ϑ_{23}	0.32	0.28	0.29
ϑ_{13}	0.32	0.28	0.29

Table 2. Fiber orientation for layup-1, layup-2 and layup-3 of hybrid composite propeller

Layup-1		Layup-2		Layup-3	
Materials	Angle (^{0})	Materials	Angle (^{0})	Materials	Angle (^{0})
S_2-Glass / Epoxy	45	S_2-Glass / Epoxy	55	S_2-Glass / Epoxy	55
S_2-Glass / Epoxy	45	S_2-Glass / Epoxy	55	S_2-Glass / Epoxy	55
Carbon / Epoxy	0	Carbon / Epoxy	0	Carbon / Epoxy	90
Carbon / Epoxy	0	Carbon / Epoxy	90	Carbon / Epoxy	0
Carbon / Epoxy	0	Carbon / Epoxy	90	Carbon / Epoxy	0
Carbon / Epoxy	0	Carbon / Epoxy	0	Carbon / Epoxy	90
R-Glass / Epoxy	90	R-Glass / Epoxy	45	R_Glass / Epoxy	45
Carbon / Epoxy	45	Carbon / Epoxy	0	Carbon / Epoxy	90
Carbon / Epoxy	0	Carbon / Epoxy	90	Carbon / Epoxy	0
Carbon / Epoxy	0	R-Glass / Epoxy	0	Carbon / Epoxy	90
R-Glass / Epoxy	-45	R-Glass / Epoxy	45	R_Glass / Epoxy	45
Carbon / Epoxy	0	R-Glass / Epoxy	0	Carbon / Epoxy	90
Carbon / Epoxy	90	R-Glass / Epoxy	45	Carbon / Epoxy	45
R-Glass / Epoxy	45	Carbon / Epoxy	0	R_Glass / Epoxy	90
Carbon / Epoxy	0	Carbon / Epoxy	90	Carbon / Epoxy	0
R-Glass / Epoxy	0	Carbon / Epoxy	0	R_Glass / Epoxy	90

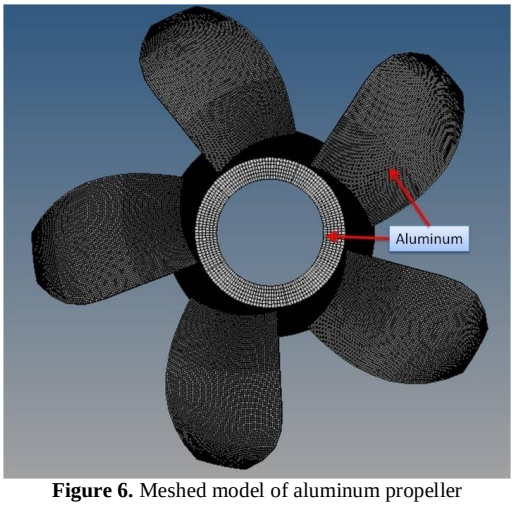

Figure 6. Meshed model of aluminum propeller

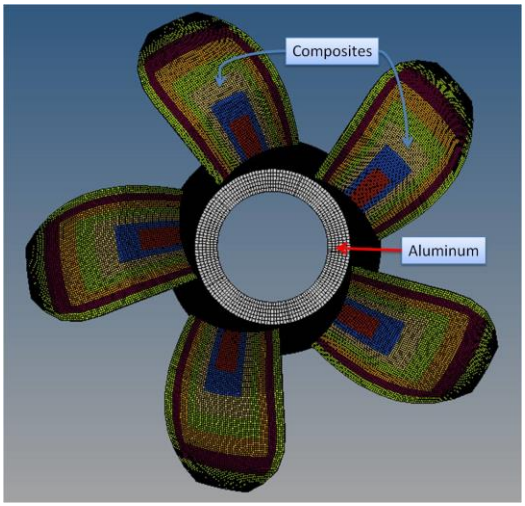

Figure 7. Meshed model of composite propeller

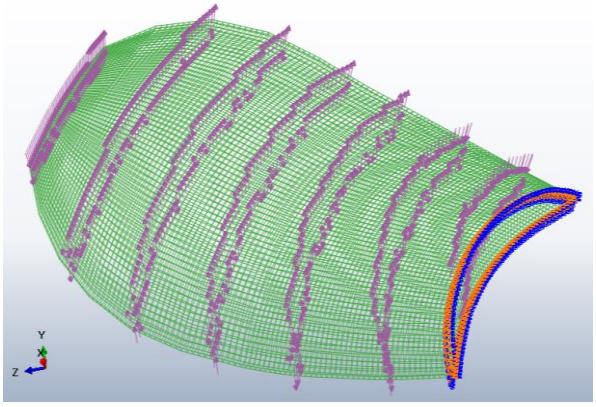

Figure 8. Fluid pressure applied on propeller blade in Abaqus

4. Results and discussion

Fluid flow analysis was carried out on propeller using Fluent to find the pressure loads on the blades when propeller is rotating at a speed of 780 rpm and these pressure loads were exported into Abaqus for fluid structure interaction analysis to find the strength of aluminum propeller and hybrid composite propeller with three different layup sequences. Solution is initiated from inlet of propeller and it is converged after 2000 iterations. The validation of present simulation methodology was carried out by comparison of non-dimensional coefficients such as thrust coefficient (K_T) and torque coefficient (K_Q) with experimental results and found that there is a good agreement between the simulation and experimental results obtained from cavitation tunnel [4]. The torque and thrust force of propeller obtained from CFD simulations at present boundary conditions are 93.62 N-m and 3002.5 N respectively.

Figure 9 and Figure 10 show the static pressure and velocity on the face and back sides of propeller blade respectively. From the results it is observed that the maximum pressure is observed at middle of blade and minimum pressure is observed at ends of propeller blade. The maximum pressure of 0.97MPa observed at the center of blade. The pressures on the blades varied from 0.15MPa to 0.97MPa. The maximum velocity of 30.3 m/sec observed at the tip of blade and minimum velocity observed at the nose cone. The surface velocity on face of the propeller varied from 1.53 m/sec to 30.3 m/sec.

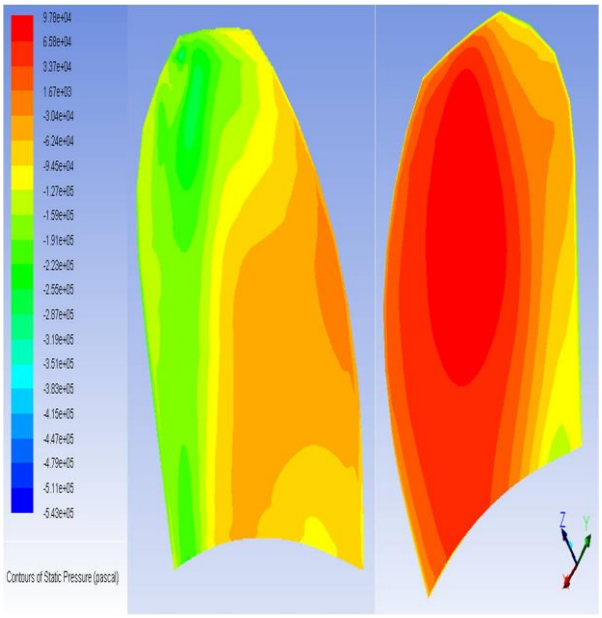

Figure 9. Static pressure (Pa) on face and back side of propeller

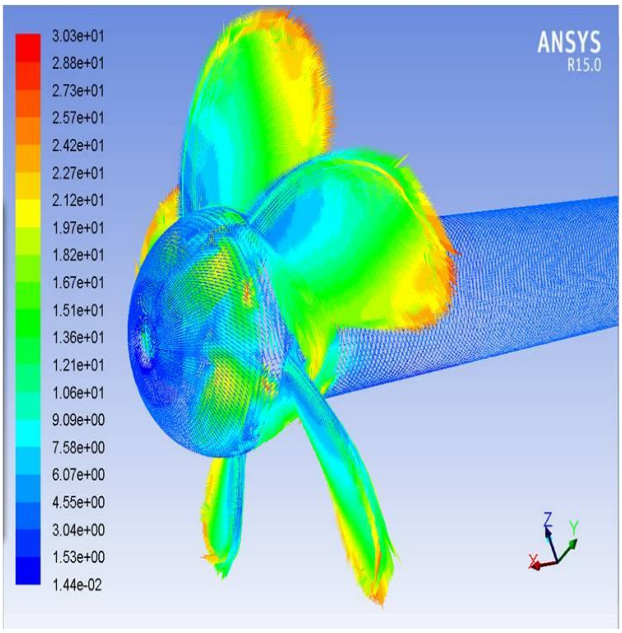

Figure 10. Velocity on propeller face (m/s)

The greatest tensile stress and deflection in aluminum propeller are 5.4 MPa and 0.434 mm respectively. From the static analysis on hybrid composite propeller with layup-1, it is observed that

percentage decrease of longitudinal stress, transverse stress and shear stress is 44.4%, 46.8% and 55.5% respectively when compared with aluminum propeller. And also there is an increase of 96.7% deflection in hybrid composite propeller with layup-1, when compared with aluminum propeller. Improved deflection in layup-1 providing the more viscoelastic damping energy. It is an encouraging results for damping of structural vibrations in composite propeller when compared with aluminum propeller. The reduction of vibration levels leads to the reduction of noise and also improve the cavitation performance in hybrid composite propeller when compared with aluminum propeller.

The percentage decrease of longitudinal stress is 52.0% in hybrid composite propeller with layup-2 when compared with aluminum propeller. Transverse and shear stress are reduced to 63.0% and 65.2% respectively in hybrid composite propeller with layup-2 when compared with aluminum propeller. Longitudinal stress, transverse stress and shear stress in composite propeller with layup-3 are further reduced by 21.1%, 31.2% and 24.2% respectively when compared with hybrid composite propeller with layup-1. Hybrid composite propeller with layup-3 shows an encouraging result when compared with hybrid composite propeller with layup-1 and layup-2. Figure 11 show the stresses on hybrid composite propeller with layup-3.

Table 3 shows the stresses and deflection on aluminum and hybrid composite propeller obtained from fluid structural analysis using Abaqus. From the results it is observed that greatest stress is observed in aluminum propeller and least stress is observed in hybrid composite propeller with layup-3. The greatest defection is observed in composite propeller with layup-1 and least deflection is observed in composite propeller with layup-3. From these fluid structure interaction studies on aluminum propeller and hybrid composite propeller with three different layups, it is observed that hybrid composite propeller with layup-3 is the better choice for the present case.

Table 3. Stresses and deflection on aluminum and composite propeller

	Aluminum	Layup-1	Layup-2	Layup-3
Stresses in longitudinal direction of blade(MPa)	5.408	3.003	2.594	2.369
Stresses in transverse direction of blade (MPa)	10.32	5.486	3.817	3.776
Shear stress (MPa)	3.665	1.629	1.277	1.234
Deflection (mm)	0.434	0.854	0.416	0.371

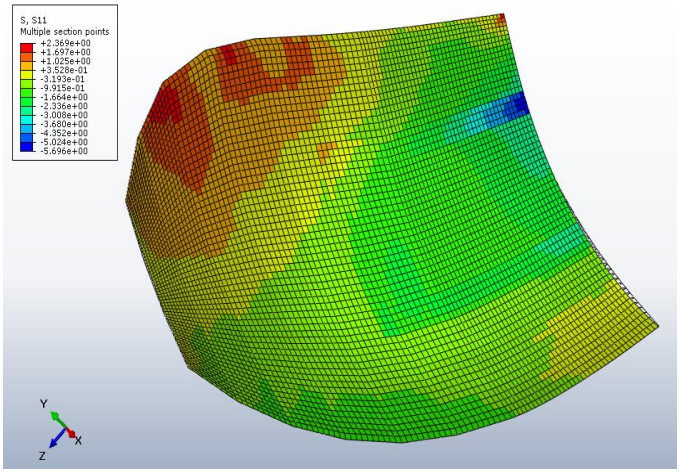

Figure 11. Stresses in hybrid composite propeller with layup-3

Damage initiation analysis was carried out on hyrid composite propeller with optimized layup-3 as per the for Hashin damage criteria available in Abaqus to check initiation of damage in the first ply. The Hashin damage criteria analysis was carried out using damage initiation mechanisms like fiber tension, matrix tension, fiber compression and matrix compression. Figure 12 and Figure 13 show fiber and matrix tension with Hashin damage criteria respectively. From the evaluation of damage model based on Hashin damage criteria for four different damage initiation mechanisms using Abaqus, it is observed that the maximum value of Hashin damage criteria variable does not exceed 1.0, which indicates that the design is safe for applied pressure loads on the hybrid composite propeller with layup-3.

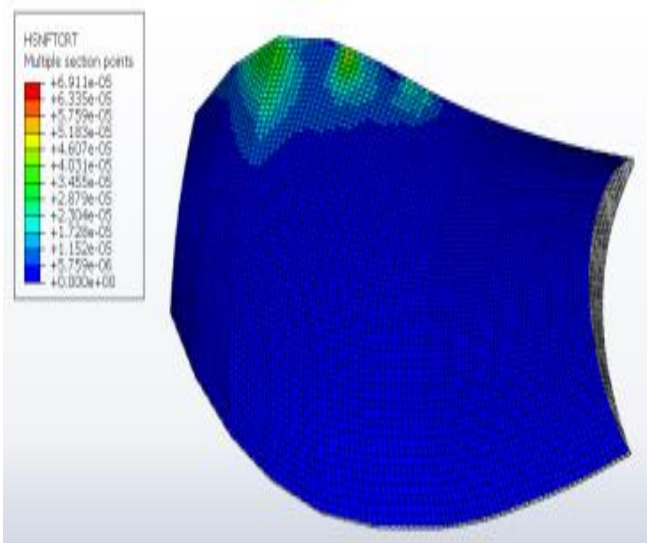

Figure 12. Fiber tension with Hashin damage criteria

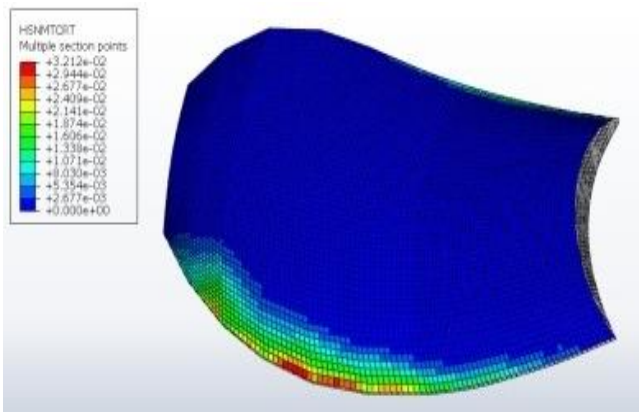

Figure 13. Matrix tension with Hashin damage criteria

5. Conclusions

Fluid structure interaction studies are carried out on hybrid composite marine propeller with different layup orientations. The stresses generated in the hybrid composite propeller are compared with aluminum propeller to quantify the reduction of stress. From the fluid structure interaction analysis, it is found that the hybrid composite propeller designed with layup-3 generates least stress compared with other designs. From these results, it was observed that normal stress and shear stress are reduced by 43.8 % and 33.6% in hybrid composite propeller designed with layup-3 when compared with aluminum propeller. The damage initiation check analysis was carried out using Hashin damage criteria available in Abaqus for fibre/matrix in tension/compression and found that the design is safe. From the analysis it is concluded that hybrid composite marine propeller designed with Carbon/R-Glass/S_2-Glass fiber and layup sequence of $55^0/55^0/90^0/0^0/0^0/90^0/45^0/90^0/0^0/90^0/45^0/90^0/45^0/90^0/0^0/90^0/0^0$ is the best choice for reduction of weight and noise, to increase the strength and to improve the performance in cavitation and corrosion when compared with baseline aluminum propeller.

References

[1] Morteza Ha., Mirzabozorga M.A.S., Bazazzadeh M., 2019, Numerical study of the effect of the tip gap size and using a single circumferential groove on the performance of a multistage compressor, Journal of Computational Applied Mechanics 50(1): 54-62.

[2] Fazel D., Kadivar M. H., Zohoor H., Hematiyan M., Farid M.R., 2019, Failure procedure in adhesive composite joints under different types of loading, Journal of Applied and Computational Mechanics 5(4): 647-651.

[3] Donald Smith R., Slater John E., 1988, The geometry of marine propellers, Technical Memorandum 88/214: AD-A203 683, National Defence Research and Development Branch, Canada.

[4] Subhas S., Saji V.F., Ramakrishna S., Das H.N., 2012, CFD analysis of a propeller flow and cavitation, International Journal of Computer Applications 55(16): 26-33.

[5] Barry C., 2005, Propeller selection for boats and small ships, E-Marine Training - Prop Matching, 1-32.

[6] Marsh G., 2004, A new start for Marine Propellers, Reinforced Plastics 48(11): 34-38.

[7] Rahimi N., Hussain A.K., Meon M.S., Mahmud J., 2012, Capability assessment of finite element software in predicting the last ply failure of composite laminates, Procedia Engineering 41: 26-33.

[8] Rama Krishna S., Rama Krishna A., Ramji K., 2011, Reduction of motor fan noise using CFD and CAA simulations, Applied Acoustics 72(12): 982-992.

[9] Zhang Y.X., Yang C.H., 2009, Recent development in finite element analysis for laminated composite plates, Composite Structures 88(1): 147-157.

[10] Mahmud J., Ismail A.F., Pervez T., 2005, Employing a failure criterion with interaction terms to simulate the progressive failure of carbon epoxy laminates, The Institution of Engineers Malaysia 66(2): 6-14.

[11] Sathish kumar T.P., Satheesh kumar S., Naveen J., 2014, Glass fiber-reinforced polymer composites - A review, Journal of Reinforced Plastics and Composites 33(13): 1258-1275.

[12] Mohsen G., Hassan G., Jalal M., 2017, Hydrodynamic effect on the sound pressure level around the marine propeller, Indian Journal of Geo Marine Sciences 46: 1477-1485.

[13] Shishesaz M., Kharazi M., Hosseini P., Hosseini M., 2017, Buckling behavior of bomposite plates with a pre-central circular delamination defect under in-plane uniaxial compression, Journal of Computational Applied Mechanics 48(1): 111-122.

[14] https://altairuniversity.com/wp-content/upload/2014/02/meshing.pdf, 2014, Accessed 16 September 2019.

[15] Jingwei J., Cai H.M., Cheng Q., Zhengfang C., Peng K.W., 2018, A ship propeller design methodology of multi-objective optimization considering fluid–structure interaction, Engineering Applications of Computational Fluid Mechanics 12(1): 28-40.

[16] Maljaars P., Bronswijk L.M.E., Windt J., Grasso N., Kaminski M., 2018, Experimental validation of fluid–structure interaction computations of flexible composite propellers in open water conditions using BEM-FEM and RANS-FEM methods, Journal of Marine Science and Engineering 6(2): 51.

[17] Prabhu J. J., Nagarajan V., Sunny M. R., Sha O.P., 2017, On the fluid structure interaction of a marine cycloidal propeller, Applied Ocean Research 64: 105-127.

[18] Sun H., Xiong Y., 2012, Fluid-structure interaction analysis of flexible marine propellers, Applied Mechanics and Materials 226: 479-482.

[19] Zelibe C.G., Adewumi O., Onitiri A., 2019, Numerical investigation of the performance of fibre-glass/talc filled epoxy composite as insulator in heating applications, Journal of Computational Applied Mechanics, doi: 10.22059/jcamech.2019.278329.371.

[20] Das H. N., Kapuria S., 2019, Adaptive pitch control of full-scale ship composite propeller using shape memory alloy to enhance propulsive efficiency in off-design conditions, Journal of Intelligent Material Systems and Structures 30(10): 1493-1507.

[21] Kim J., Ahn B., Ruy W., 2019, Numerical analysis of orthotropic composite propellers, Journal of Ocean Engineering Technology 33(5): 377-386.